Fibers and Polymers (2026) 27:723–732
https://doi.org/10.1007/s12221-025-01256-w

Online ISSN 1875-0052
Print ISSN 1229-9197

REGULAR ARTICLE

Development of Sustainable Hydrophobic Coatings for Textiles Based on Sputtered Copper Nitride

M. Isabel Rodríguez-Tapiador[1,2] · Tamara Ruiz-Calleja[3] · Alberto Jiménez-Suárez[2,4] · Susana M. Fernández[1]

Received: 29 May 2025 / Revised: 31 October 2025 / Accepted: 12 November 2025 / Published online: 20 November 2025

Abstract

This study investigates the use of copper nitride (Cu_3N) thin films as a hydrophobic coating for acrylic textiles, offering a safer and more sustainable alternative to conventional fluorocarbon-based treatments. Copper nitride is a non-toxic, abundant, and cost-effective semiconductor material with tunable properties, yet its application in textiles remains largely unexplored. In this work, Cu_3N coatings were deposited on acrylic fabric using reactive sputtering at room temperature, 50W of power and 3.5 Pa of working pressure, under two different gas atmospheres: pure nitrogen (N_2) and a nitrogen-argon ($N_2 + Ar$) mixture. Deposition times were varied at 60, 90, and 120 min to evaluate the influence of process duration on hydrophobic performance. Hydrophobicity was assessed by measuring the water contact angle on coated samples, both in their initial state and after mechanical stress tests including washing and folding. The results demonstrated strong hydrophobic behavior across all samples, with contact angles ranging from 96.30° to 113.68°. Notably, coatings deposited under $N_2 + Ar$ showed slightly enhanced performance and durability compared to those deposited under pure N_2. The entire process was conducted at room temperature and generated no chemical waste, highlighting its environmental advantages. These findings suggest that copper nitride coatings can effectively impart hydrophobicity to textiles without relying on harmful fluorinated compounds. The combination of performance, safety, and sustainability positions Cu_3N as a promising candidate for future textile finishing technologies.

Keywords Hydrophobicity · Fabric · Copper nitride · Coating · Contact angle

1 Introduction

Hydrophobic coatings are widely used in the textile industry for various applications, including home textiles, sports apparel, and intimate garments [1]. Traditionally, these coatings have been predominantly obtained through fluorocarbon-based treatments [2], which have consistently demonstrated their effectiveness. Fluorocarbons create water-repellent surfaces due to their unique molecular structure. However, recent studies have raised concerns about the safety of these products, citing health and environmental issues [3–5]. Research has shown that fluorocarbons are extremely durable and bio-accumulative, and the longer the compound chain, the more challenging it is to degrade [2].

Fortunately, the search for sustainable alternatives to achieve hydrophobic textile surfaces is yielding promising results. One of the most important lines of research in this field is the biomaterial-based fabrication of superhydrophobic textiles [6, 7], where products such as natural wax [8, 9] and waterborne polyurethane [10, 11] confer hydrophobicity

✉ Tamara Ruiz-Calleja
tamara.ruiz@urjc.es

✉ Susana M. Fernández
susanamaria.fernandez@ciemat.es

M. Isabel Rodríguez-Tapiador
MariaIsabel.Rodriguez@ciemat.es

Alberto Jiménez-Suárez
alberto.jimenez.suarez@urjc.es

1 Departamento de Energía, CIEMAT, Av. Complutense 40, 28040 Moncloa-Aravaca, Madrid, Spain

2 Area de Ciencia e Ingeniería de Materiales, Universidad Rey Juan Carlos, Tulipán, s/n, 28933 Móstoles, Spain

3 Universidad Rey Juan Carlos, Calle Tulipán, 28933 Móstoles, Spain

4 Instituto de Investigación de Tecnologías para la Sostenibilidad, Universidad Rey Juan Carlos, c/Tulipán s/n, 28933 Móstoles, Madrid, Spain

to a wide range of textile surfaces. Plasma technology is also playing a crucial role in the development of hydrophobic finishes [12–14], due to its ability to produce rough surface micronanotextures needed for superhydrophobic surfaces [15]. Other approaches, such as closing the porosity of the fabric through melting and flowing of the yarns [16], or laser surface texturing [17], can produce durable water-repellent fabrics.

On the other hand, copper nitride (Cu_3N) is a simple binary semiconductor compound composed of environmentally friendly elements. This material is very interesting because of its non-toxicity, safely, abundance and cost-effectiveness, showing great potential in different scientific and technological applications due to its excellent properties [18]. As example, Cu_3N is being strongly considered as a promising candidate to replace conventional toxic and/or rare materials (cadmium telluride and/or copper indium gallium diselenide), giving rise to a much cleaner thin film solar cell technology [19]. This is largely due to the ease of tuning its properties simply by changing the manufacturing conditions and/or by doping with metal or non-metal elements (fluorine, gold, silver and so on), resulting in either p-type or n-type behavior [20]. Thereby, the band gap energy and the electrical properties can be adapted to the needs of a specific application. Taking this skill into account, a bright future is foreseen for the use of this material, considering scalable and low-cost manufacturing routes [21].

Despite the attractive properties of this nitride and its potential to enhance a wide range of surfaces, a comprehensive literature review reveals that it has been scarcely utilized in textile applications. Huang et al. [22, 23] explore various characteristics of fabrics coated with CuN and TiN films, demonstrating their antibacterial potential and ultraviolet protection. However, not a single paper examines the ability of copper nitride to render textile surfaces hydrophobic, highlighting the relevance of the present research.

This study explores the potential of depositing copper nitride films on acrylic fabric to achieve a hydrophobic effect. The contact angle is measured on the coatings as-is and after they have been washed and folded. Copper nitride is considered safe for human health, and the process, conducted at room temperature, generates no waste, making it environmentally friendly. Therefore, it presents an interesting alternative to harmful hydrophobic finishes, such as those containing fluorocarbons.

2 Experimental

2.1 Materials

The fabric used for this research is a 100% acrylic taffeta with a mass per unit area of 260 g/m^2 and chemically dyed in bright red, purchased from Tejidos Paredes. This specific textile is selected from an extensive catalog due to its suitability for outdoor applications, where hydrophobicity may be a desired quality. No further treatments are carried out before the coating procedure.

Cu_3N coatings are fabricated using a physical vapor deposition method by sputtering material from a commercial magnetron Cu target with a purity of 99.99% and 3-inch diameter of the Lesker Company and using N_2 (purity 99.999%) as reactive gas.

2.2 Coating Procedure

The deposition of the Cu_3N coatings is carried out using a commercial MVSystem Inc. monochamber sputtering system. This system has a vertically adjustable gun that is operated by radio-frequency (RF). The fabric is loaded into the vacuum chamber using a substrate holder to support it so that it remains completely flat, without wrinkles. The distance between the target and the textile is set to 10 cm. Prior to the coating deposition, the chamber is pumped with a turbopump to 10^{-5} Pa of base pressure. After that, both the Argon (Ar) and N_2 sputtering gases are introduced into the chamber, controlling their fluxes with mass flow controllers (MFC). In all experiments, a constant flow rate of 20 sccm of N_2 and 10 sccm of Ar was maintained, resulting in a total gas flow of 30 sccm. Based on these flow rates, two deposition conditions with different gas ratios (R) were defined. The first corresponds to a pure N_2 atmosphere ($R = 1.0$), and the second to a mixed Ar/N_2 atmosphere ($R = 0.7$), where R is defined as $R = [N_2/(Ar + N_2)]$. The working sputtering pressure is set to 3.5 Pa, value adjusted with a "butterfly" valve. The Cu_3N coatings are deposited at room temperature (RT), with non-intentional heating, at a fixed RF power of 50W. The deposition time is varied from 3600 to 7200 s. The estimated deposition rate for the coatings deposited in the $N_2 + Ar$ was 0.11 nm/s, while for those deposited in N_2, it was 0.07 nm/s [24].

Table 1 shows the main sputtering deposition conditions used in the coatings of the textile samples.

2.3 Samples Characterization by Scanning Electron Microscopy (SEM)

SEM was performed on the coated cross-section of the acrylic fabrics once coated to see if any alterations on the geometry or disposition were observed. This is very important as the modification of the fabrics may lead to the alteration of their behavior, such as wettability of the surface. The equipment used was a SEM S-3400N model from Hitachi (Tokyo, Japan) and the images were taken in secondary electrons mode to observe just morphological aspects. The images were taken with an acceleration potential of 15 kV

Table 1 Sputtering deposition conditions of the coating process and samples nomenclature

Code sample	Partial N_2 pressure (R)	Deposition time (min)
As coated samples		
M1	1.0	60
M2	1.0	90
M3	1.0	120
M4	0.7	60
M5	0.7	90
M6	0.7	120
Washed and folded samples		
ML-1	1.0	60
ML-2	1.0	90
ML-3	1.0	120
ML-4	0.7	60
ML-5	0.7	90
ML-6	0.7	120

over the samples coated with a 1.8–2.5 nm Au layer to avoid electric charge of the samples.

2.4 X-Ray Diffraction

To evaluate the crystallinity of the Cu_3N film on the fabric substrate, the sample processed at 3.5 Pa with an Ar/N_2 gas mixture is studied using X-ray diffraction (XRD). The analysis is conducted using a commercial system (model PW3040/00 X'Pert MPD/MRD) from Malvern Panalytical Ltd. (Malvern, UK), with Cu-Kα radiation (λ = 0.15406 nm). The measurement covers a 2θ range from 10° to 60°, with a step interval of 0.01° and a time step of 20 s.

2.5 Wettability

Wettability is evaluated by measuring the contact angle of distilled water droplets on the surface of the fabric using Rame-Hart 200 contact angle goniometer. Images are later analyzed using image processing software ImageJ. Three drops are deposited for each trial, and the average angle is obtained. The wettability of the samples is measured in three cases: (a) as-coated samples; (b) after a 45-min washing cycle at 20 °C and 1400 rpm; (c) after being folded one hundred times along the same line, depositing the drop on the fold line.

2.6 Fourier Transform Infrared (FT-IR) Analysis

FT-IR spectroscopy is carried out with a Perkin Elmer Spectrum 100 FT-IR in the range of 500–4000 cm^{-1} in transmittance mode to provide a rapid 'chemical fingerprinting' of the coatings thanks to its interaction with the IR radiation.

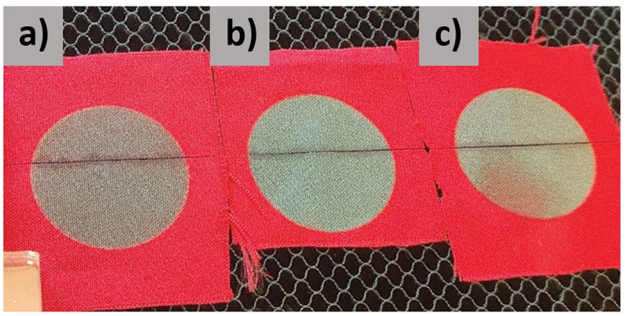

Fig. 1 Samples: **a** M3; **b** M2; **c** M1, after being laser cut

3 Results and Discussion

After visual inspection, no visible degradation of the textile is observed following the coating procedure and all regions appear evenly coated after the sputtering process. At a macroscopic scale, the coated samples exhibited a copper-colored layer that darkens as the deposition time increased, as seen in Fig. 1. Since the base fabric is red, it is evident that the coating is opaque. No visual differences were observed at first appearance between the samples.

3.1 X-Ray Diffraction

XRD measurements were conducted on the sputtered fabricated Cu_3N coatings on the fabric to characterize their main structural properties, and to determine the possible variations in them due to the sputtering conditions used, and the post-treatment applied based on washing and folding. The XRD patterns of the as-deposited and treated coatings are depicted in Fig. 2. These spectra confirmed the polycrystalline nature of the Cu_3N, which exhibited the typical anti-ReO_3 crystal structure (card number 00.047.1088) showed in our previous studies by the material deposited on rigid substrates [21, 25]. It can be appreciated that all the samples presented the characteristics peaks of Cu_3N related with the (100), (111), and (200) planes. The preferred orientation seems to be apparently the (100) plane, what is difficult to determine because this diffraction peak is masked by the amorphous halo of the acrylic taffeta. [26]. After washing and bending, no significant variation in the position of the peaks was observed, which allows assuming that the coating remains stable on the acrylic fibers.

The grain size (τ) and the microstructural strain (ε) were extracted from the XRD measurements using the Debye–Scherrer (1) and Debye (2) equations, respectively

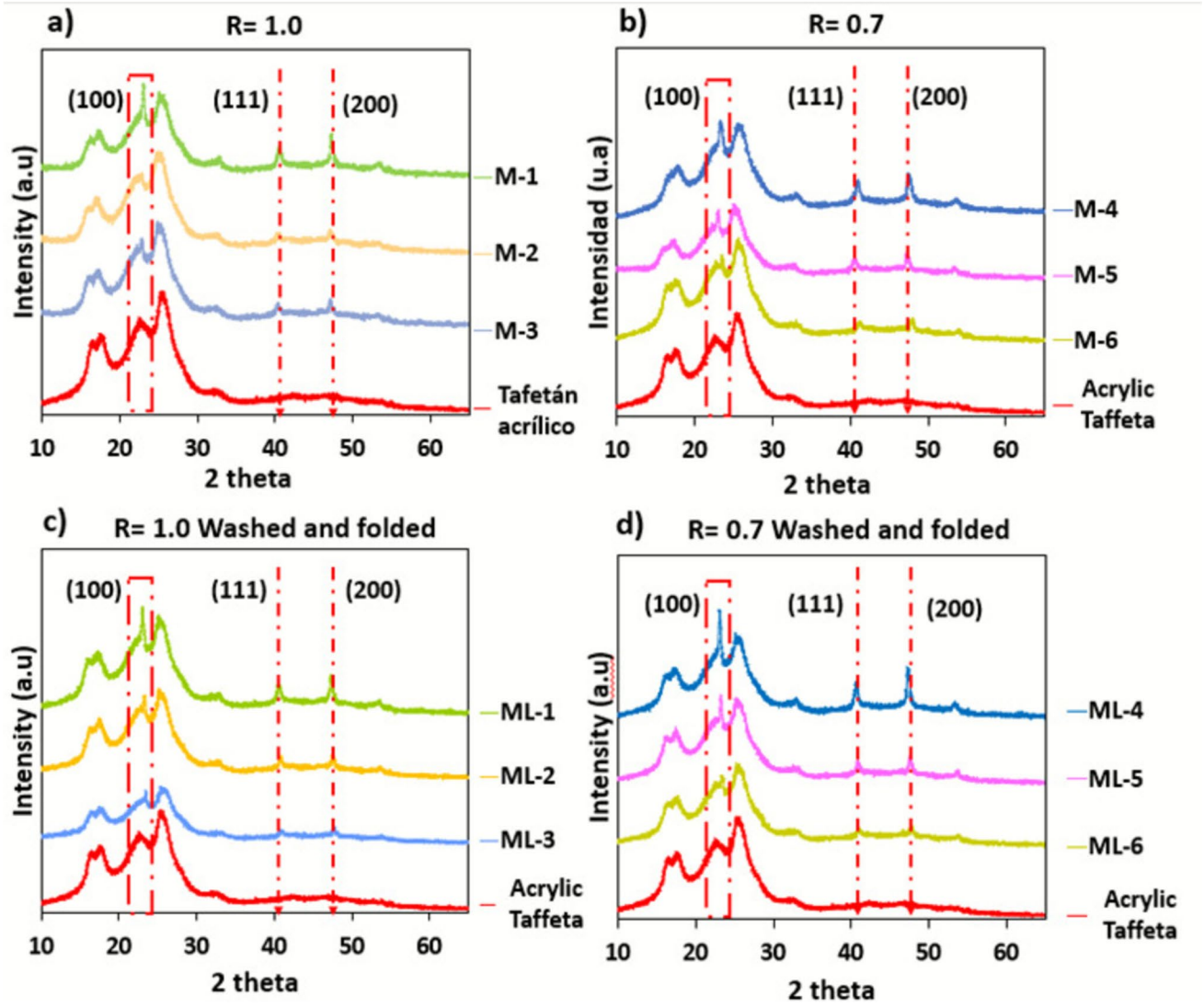

Fig. 2 XRD spectra: **a** $R = 1.0$ as coated; **b** $R = 0.7$ as coated, **c** $R = 0.1$ after washing and folding, **d** $R = 0.7$ after washing and folding

$$\tau = \frac{K\lambda}{\beta \cdot \cos\theta}, \tag{1}$$

$$\varepsilon = \frac{\beta \cdot \cot\theta}{4}, \tag{2}$$

where K is a constant (~0.9), λ is the X-rays wavelength (0.15406 nm), θ is the diffraction angle, and β is the full width at half maximum (FWHM) of the analyzed orientation [27, 28]. These preliminary results indicate that the initial structural quality of the coating directly influences its functional stability. This will be corroborated later with FT-IR and SEM measurements.

It can be observed in Table 1 that the values of the FWHM and the grain size were lower and higher, respectively, when using a pure N_2 atmosphere, being slightly influenced by the deposition time. This is in accordance with our previous studies obtained over glass substrates [21]. That fact would be indicative of an improved crystalline quality obtained in the coatings fabricated under those sputtering conditions. On the other hand, the ε increased when Ar was introduced in the atmosphere. This can be attributed to hindered formation of the Cu_3N layer, which would lead to a more defect presence and a structural disorder that would interrupt the grain growth, generating a more stressed lattice. These effects suggest a greater internal stress in the films induced by the presence of Ar in the atmosphere [25].

After washing and bending the samples, those parameters (Table 2) were strongly affected. This effect was mainly observed at higher deposition times, while the coating deposited under the pure N_2 atmosphere and the shortest deposition time of 60 min remained almost unaffected.

Table 2 FWHM, grain size, and microstructural strain, calculated from the XRD spectra

Code sample	Partial N_2 pressure (R)	FWHM (°)	τ (nm)	ε
M1	1.0	0.1378	59	2.95×10^{-3}
M2	1.0	0.1349	60	2.92×10^{-3}
M3	1.0	0.1378	59	2.97×10^{-3}
M4	0.7	0.1968	41	4.18×10^{-3}
M5	0.7	0.1968	41	4.23×10^{-3}
M6	0.7	0.1574	52	3.30×10^{-3}
Washed and folded sample				
ML-1	1.0	0.1378	59	2.96×10^{-3}
ML-2	1.0	0.2165	37	4.58×10^{-3}
ML-3	1.0	0.5940	14	1.25×10^{-2}
ML-4	0.7	0.2165	37	4.63×10^{-3}
ML-5	0.7	0.6200	13	1.31×10^{-2}
ML-6	0.7	0.2755	29	5.78×10^{-3}

These preliminary results indicate that the initial structural quality of the coating directly influences its functional stability. This will be corroborated later with FT-IR and SEM measurements.

3.2 SEM Characterization

Figure 1 shows the SEM images of samples coated at different partial pressure of N_2, both as-is (Fig. 3a–f) and after a washing cycle (Fig. 3g–l), to analyze the influence of the coating process on the textile. In its initial state, the acrylic taffeta (not shown here) presents an intertwined textile architecture, with fibers of uniform section and surface porosity, typical of the polymeric material. After coating, no significant differences were found between samples at the microscopic level, and the coating replicated the shape of the material on which it is deposited. In addition, the coating was only observed on the fibers, that is, the space between fibers and tows is kept, which is very important for wearable fabrics. The samples deposited at $R=0.7$ (Fig. 3a–c) exhibited a non-continuous coating, with low coverage areas and incipient microcracks. This is coherent with the higher

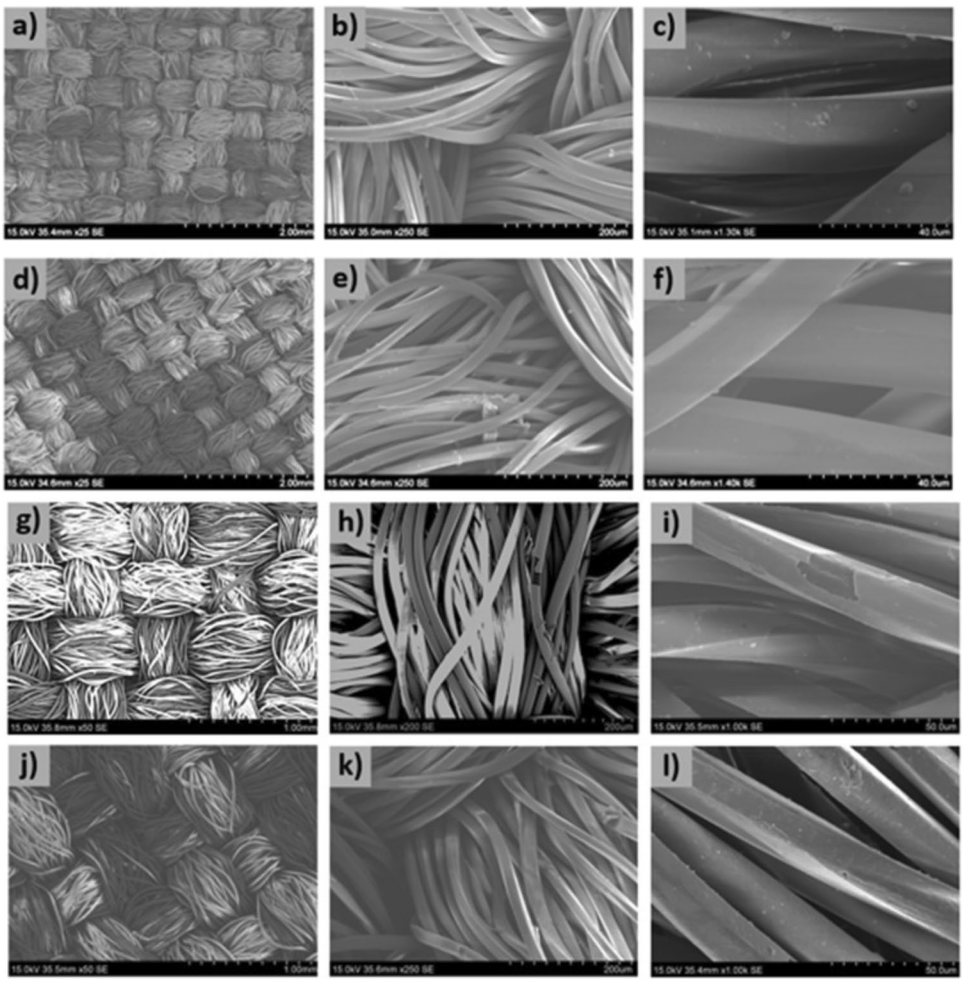

Fig. 3 SEM images: **a–c** samples $R=0.7$; **d–f** samples $R=1.0$ before washing and bending; **g–i** after washing and bending with $R=0.7$, and **j–l** after washing and bending with $R=1.0$

ε values obtained in XRD for these samples, indicative of an internal stress (see data in Table 2) that would lead to its rupture. In addition, it could be attributed to a less efficient formation of a Cu_3N phase, along with a weak adhesion to the substrate. In contrast, the samples deposited at $R = 1.0$ (Fig. 3d–f) showed a uniform and continuous coating, apparently without the formation of significant cracks, suggesting a good nucleation and growth under these conditions. In both cases ($R = 0.7$ and $R = 1.0$), the presence of what appears to be Cu_3N agglomerations, randomly distributed, were observed.

After the washing and folding treatments, the samples fabricated at $R = 1.0$ (Fig. 3j–l) showed localized degradation. Although most of the coating remained adhered, areas with cracks and partial detachment were observed, especially in folding regions. This degradation can be attributed to the repeated mechanical action and the abrasiveness of washing. Despite mechanical wear, the overall coverage remained reasonably uniform, indicating good initial adhesion. On the other hand, the coatings deposited at $R = 0.7$ (Fig. 3g–i) showed a more severe damage. Areas with evident peeling, extensive cracks, and complete discontinuity of the coating were observed. The initial fragility of the film, combined with the poor coverage, appeared to favor its detachment under mechanical stress. Specifically, in Fig. 3i, l, it can be observed that washing can cause a slight increment of the size of the imperfections observed prior to washing (Fig. 3c, f), while the overall coating was kept homogeneously distributed on the fabric. These results indicate that the partial N_2 pressure, R, would critically influence the quality and stability of the coating. Therefore, the sputtering conditions of $R = 1.0$ seem to generate more homogeneous and resistant layers, while those deposited at $R = 0.7$ would lead to more fragile and discontinuous films. These results highlight that for functional textile applications, where mechanical strength and durability are required, optimizing both the stoichiometry and microstructure of Cu_3N is indeed essential.

3.3 Fourier Transform Infrared (FT-IR) Analysis

Figure 2 shows the FT-IR spectra of the samples fabricated under the different atmospheres, before and after washing. All the samples exhibited a single band around 650 cm^{-1}, confirming the Cu–N bond formation (highlighted in the spectra). As is reported in literature [30], the Cu_3N compound exhibits a prominent peak at 652 cm^{-1} when the amount of N is adequate to form the Cu_3N phase. As it can be observed, when used $R = 0.7$, this main peak was slightly displaced, which suggest that the formation of the Cu_3N could be less uniform and may present a less orderly structure, in agreement with the XRD data shown previously in Table 2. When washed and bent (Fig. 4c, d), the spectra of each sample were not substantially modified, which could confirm that the coating was not strongly modified during both post-treatments. The increase on the defects and cracks of the coatings during the washing and bending processes observed by SEM can be corroborated by the appearance of the FT-IR double peak at around 2900–2940 cm^{-1}, attributed to the C–H stretching on the organic molecules of the acrylic fibers. The appearance of these bands after washing could be due to a greater exposure of the textile surface because of a deterioration or a partial loss of the Cu_3N coating.

3.4 Wettability

Figure 5 displays a picture of sample M2 where it can be appreciated that the uncoated fabric absorbs the drop, causing it to spread, while the drop deposited on the coating remains spherical and is not absorbed. At first glance, a very significant difference in the wettability behavior of the coated fabric compared to the uncoated fabric was observed.

The duration of the water droplet remained on the surface of the coated fabric after the washing and the folding was also determined and compared to that it took for the droplets to disappear on the uncoated fabric. It was found that the material continued to maintain its hydrophobic properties for 12 min, compared to the 4 s, time that the droplet took to be absorbed by the uncoated fabric.

Figure 4 compiles the average values obtained for the contact angle of each sample: as-is, after washing, and after folding. Both sets of samples achieved a slightly greater contact angle with longer coating times, with $105.25 \pm 2.08°$ for sample M3 and $113.46 \pm 6.10°$ for sample M6. However, the contact angles obtained by as-deposited samples at $R = 0.7$ were significantly higher than those obtained by those at $R = 1$. In our previous work [29], the chemical composition in these coatings deposited on rigid substrates was determined. The Cu/N ratio was close to the stoichiometry, being slightly lower for the samples at $R = 0.7$. This shows that these small variations in composition are not enough to explain the different hydrophobic behavior of the coatings. In this sense, this could be due to the differences in the surface topography with nanometer scale patterns (roughness and imperfections) that could promote higher contact angles. This would be in agreement with the fact that higher deposition times led to increased contact angles (Fig. 6).

After washing, the contact angles obtained by the samples deposited at $R = 0.7$ remained quite close to the values showed by the samples as-is. However, in the case of the coatings at $R = 1.0$, this tendency was different. From Fig. 6, M2 drastically improved their hydrophobicity after washing, with an increase of 124.61%. FT-IR and XRD did not provide any chemical change during the washing process. Not even the typical Cu–O peak that could form in the presence of water in an alkaline environment was observed. Taking this into account, the effects promoted

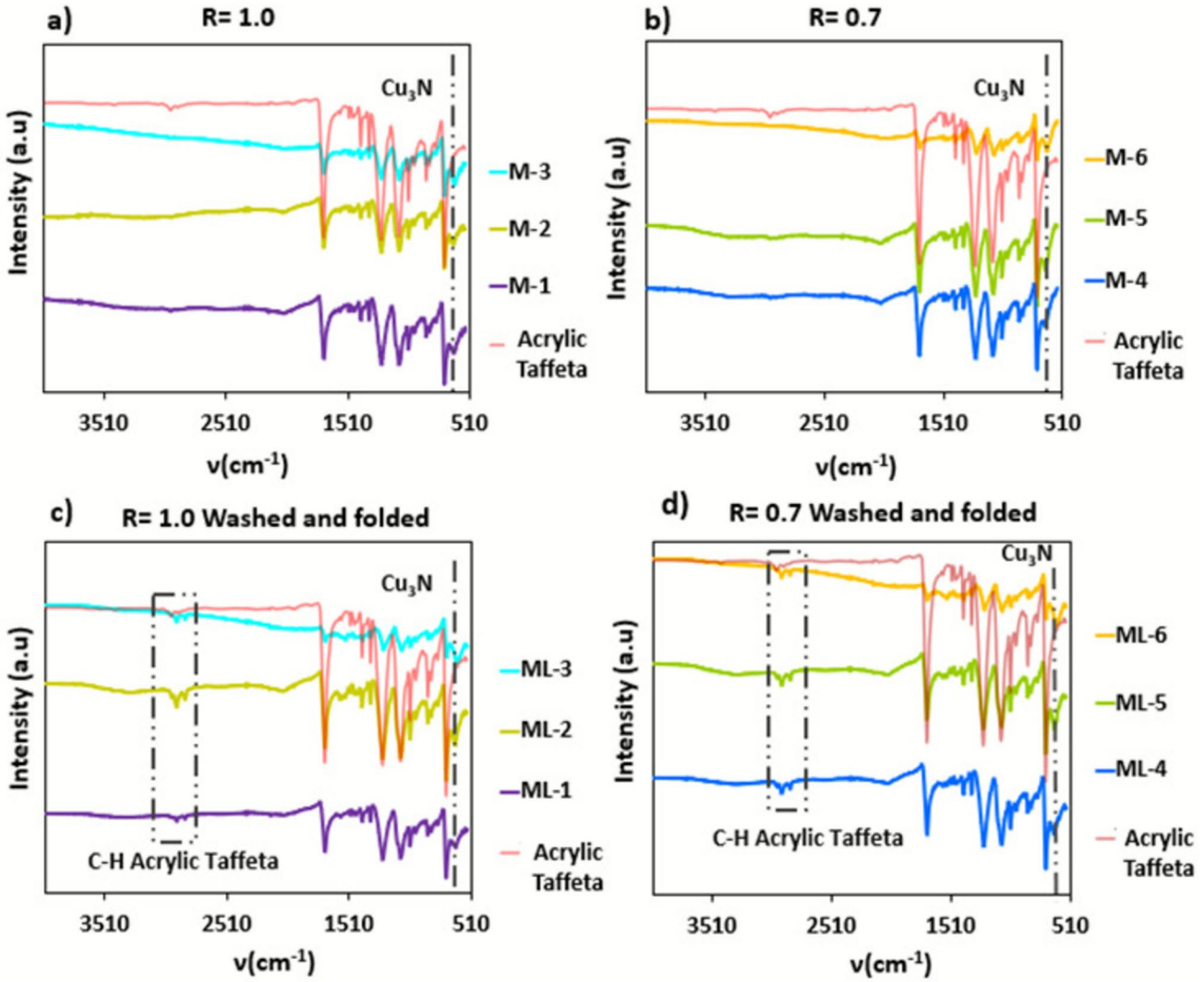

Fig. 4 FT-IR spectra of coated samples at different partial N_2 pressures before (**a**, **b**) and after washing and bending (**c**, **d**)

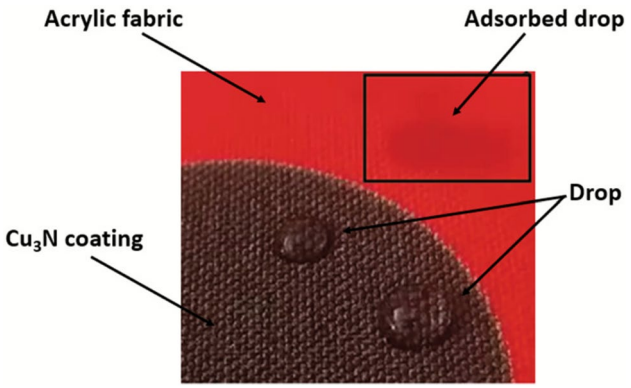

Fig. 5 Comparison of the behavior of the drop on the coated (sample M2) and the uncoated fabric

during washing could be both the increase of roughness and the partial coating deterioration. These phenomena can be aligned with the observed increase in the contact angle when the deposition time increased or even the atmosphere was based on a mixture of Ar/N_2. When measuring the contact angle on the fold line, the samples M4 to M6 once again presented similar values to the samples as-is, while samples M1 to M3 experienced a significant improvement. This can be attributed again to the formation of a surface roughness pattern that would promote a modification of the contact angle, which was already initially created when the $R = 0.7$ was used, thus being less affected by the washing and bending processes.

Figure 7 shows the comparison between the deposition of a drop on samples M3 and M6, in their as-is state, after washing, and after folding. Future investigations on this topic should include testing on different fabrics and a

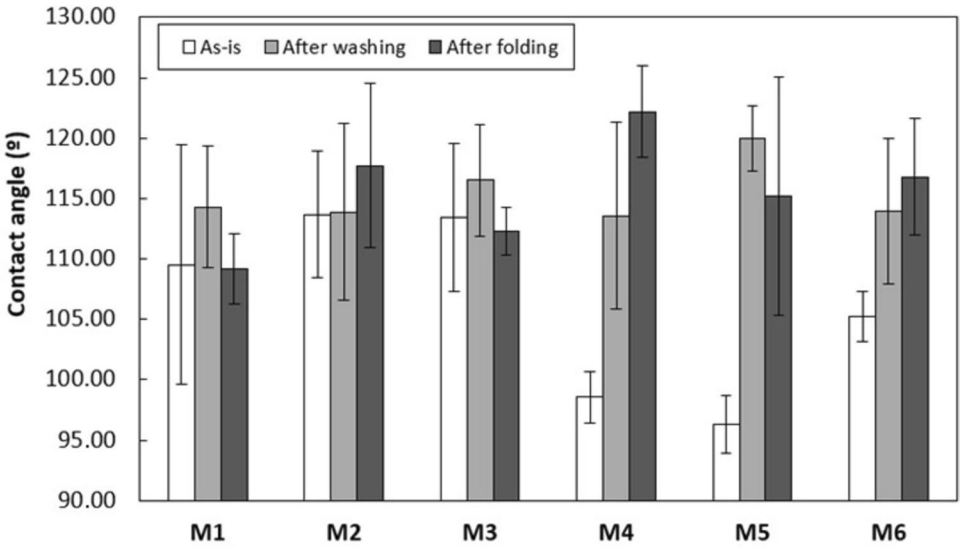

Fig. 6 Contact angle measured on the surface of the samples in study

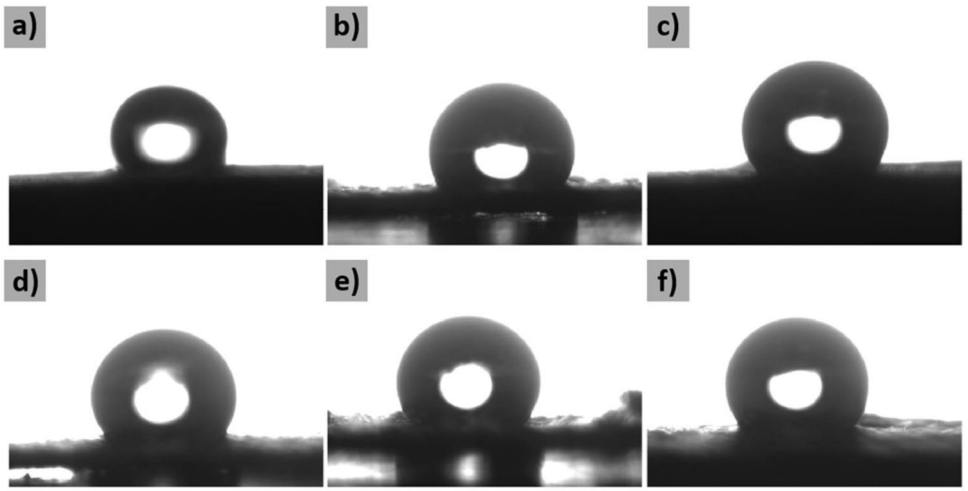

Fig. 7 **a** Sample M3 as-is, **b** sample M3 after a washing cycle, **c** sample M3 after folding, **d** M6 as-is, **e** M6 after a washing cycle; **f** M6 after folding

detailed analysis of the durability of the coating, involving more washing cycles and tests such as rubbing fastness.

All these results corroborate that the coating fabricated at $R = 1.0$ is the most stable, and therefore it remains more unchanged after mechanical treatments. Based on these data, it appears to be optimal from a production and in service life point of view.

4 Conclusion

In this work, an acrylic fabric was coated with copper nitride fabricated by reactive magnetron sputtering technique. In this sense, the process and the material used for the coating can be considered safe for both the health and the environment. This is because they are processed using a technique that involves low energy consumption, since the films can be manufactured at RT, without the use of toxic gases and/or the production of waste. Under this perspective, the coatings showed in this work could be considered as an excellent alternative for improving the hydrophobicity of acrylic textiles, without the use of more harmful toxic coatings, as those based on fluorocarbons. The main conclusions drawn from these experiments include:

The as-deposited Cu_3N coatings provided hydrophobicity to the surface of the fabric, achieving contact angles ranging between 96.30° and 105.25° for the samples fabricated with a pure N_2 atmosphere, and between 109.54° and 113.68°, for the samples with Ar/N_2.

After a washing cycle and one hundred folding cycles, the samples fabricated in a pure N_2 atmosphere experienced a significant improvement in their hydrophobicity, reaching an improvement up to 124.61%, while the samples produced in an Ar/N_2 atmosphere did not show such huge improvement, mainly attributed to their greater fragility.

The duration of the droplet on the treated fabric was around 12 min, unlike the 4 s it took to be absorbed by the fabric.

The contact angle values obtained in this work do not seem to exceed those reported in the literature for other compounds [31–33]. However, the main advantage of using Cu_3N as coating in this technology lies in the fact that it is a compound based solely on non-toxic and abundant elements (copper and nitrogen), and also that it can be deposited using processes compatible with the conventional textile technology, without the need for aggressive heat treatments or fluorinated substances. While the durability of the proposed treatment is limited, this work introduces an innovative approach to textile hydrophobicity and lays the groundwork for future optimization.

Supplementary Information The online version contains supplementary material available at https://doi.org/10.1007/s12221-025-01256-w.

Acknowledgements The authors would like to thank to the Centro de Apoyo Tecnológico (CAT) from Universidad Rey Juan Carlos for the DRX testing in their facilities.

Funding Open Access funding provided thanks to the CRUE-CSIC agreement with Springer Nature. This work was partially supported by Project Impulso 2025/00014/011, funded by Universidad Rey Juan Carlos. Project TED2021-131102B-C21, funded by MCIN/AEI/10.13039/501100011033 and the European Union "NextGenerationEU"/PRTR. Project PID2022-138496OB-I00 from Agencia Estatal de Investigación of Spanish Government. M.I.R.T. acknowledges the partial funding received from MEDIDA C17.I2G: CIEMAT. Nuevas tecnologías renovables híbridas, Ministerio de Ciencia e Innovación, Componente 17 "Reforma Institucional y Fortalecimiento de las Capacidades del Sistema Nacional de Ciencia e Innovación". Medidas del plan de inversiones y reformas para la recuperación económica, funded by the European Union—NextGenerationEU.

Data Availability Data are available upon request.

Declarations

Conflict of Interest The authors declare no conflict of interest.

References

1. L.V. Haule, L. Nambela, Advances in waterproof technologies in textiles, in *Functional and Technical Textiles*. (Elsevier, New York, 2023), pp.275–291
2. U. Sayed, P. Dabhi, Finishing of textiles with fluorocarbons. Waterproof Water Repel. Text. Cloth. (2014). https://doi.org/10.1016/B978-0-08-101212-3.00006-X
3. R. Lohmann, R.J. Letcher, The universe of fluorinated polymers and polymeric substances and potential environmental impacts and concerns. Curr. Opin. Green Sustain. Chem. **41**, 100795 (2023). https://doi.org/10.1016/j.cogsc.2023.100795
4. Z. Abunada, M.Y.D. Alazaiza, M.J.K. Bashir, An overview of per- and polyfluoroalkyl substances (PFAS) in the environment: source, fate, risk and regulations. Water **12**(12), 3590 (2020). https://doi.org/10.3390/w12123590
5. M.A. Muñoz, P.J. Lein, Toxic textiles: potential health risks associated with toxic chemicals in clothing. Open Access Gov. **41**, 384–385 (2024). https://doi.org/10.56367/OAG-041-9857
6. M. Shahid, S. Maiti, R.V. Adivarekar, S. Liu, Biomaterial based fabrication of superhydrophobic textiles – a review. Mater. Today Chem. **24**, 100940 (2022). https://doi.org/10.1016/J.MTCHEM.2022.100940
7. M. Ghasemlou, F. Daver, E.P. Ivanova, B. Adhikari, Bio-inspired sustainable and durable superhydrophobic materials: from nature to market. J. Mater. Chem. A Mater. **7**, 16643–16670 (2019). https://doi.org/10.1039/C9TA05185F
8. A. Bashari, A.H.S. Koohestani, N. Salamatipour, Eco-friendly dual-functional textiles: green water-repellent & anti-bacterial. Fibers Polym. **21**, 317–323 (2020). https://doi.org/10.1007/s12221-020-9568-6
9. N. Forsman, L.-S. Johansson, H. Koivula, M. Tuure, P. Kääriäinen, M. Österberg, Open coating with natural wax particles enables scalable, non-toxic hydrophobation of cellulose-based textiles. Carbohydr. Polym. **227**, 115363 (2020). https://doi.org/10.1016/j.carbpol.2019.115363
10. B. He, X. Hou, Y. Liu, J. Hu, L. Song, Z. Tong, X. Zhan, Y. Ren, Q. Liu, Q. Zhang, Design of fluorine-free waterborne fabric coating with robust hydrophobicity, water-resistant and breathability. Sep. Purif. Technol. **311**, 123308 (2023). https://doi.org/10.1016/j.seppur.2023.123308
11. M. Dai, Y. Zhai, Y. Zhang, A green approach to preparing hydrophobic, electrically conductive textiles based on waterborne polyurethane for electromagnetic interference shielding with low reflectivity. Chem. Eng. J. **421**, 127749 (2021). https://doi.org/10.1016/j.cej.2020.127749
12. A. Zille, Plasma technology in fashion and textiles. Sustain. Technol. Fash. Text. (2020). https://doi.org/10.1016/B978-0-08-102867-4.00006-2
13. I. Belhaj Khalifa, N. Ladhari, Hydrophobic behavior of cotton fabric activated with air atmospheric-pressure plasma. J. Text. Inst. **111**, 1191–1197 (2020). https://doi.org/10.1080/00405000.2019.1688907
14. C. Tudoran, M. Roşu, M. Coroş, A concise overview on plasma treatment for application on textile and leather materials. Plasma Process. Polym. (2020). https://doi.org/10.1002/ppap.202000046
15. E. Eslami, R. Jafari, G. Momen, A review of plasma-based superhydrophobic textiles: theoretical definitions, fabrication, and recent developments. J. Coat. Technol. Res. **18**, 1635–1658 (2021). https://doi.org/10.1007/s11998-021-00523-8
16. V. Arumugam, A.I.Y. Tok, V. Lipik, A novel method to produce sustainable wind resistant and water repellant fabric for outdoor sport clothing. J. Ind. Text. (2023). https://doi.org/10.1177/15280837231184256

17. W.-S. Chu, M.M. Shehroze, N.G. Tran, T. Dinh, S.-T. Hong, D.-M. Chun, Green fabrication of superhydrophobic surfaces using laser surface texturing without toxic chemicals: a review. Int. J. Precis. Eng. Manuf. **25**, 1101–1123 (2024). https://doi.org/10.1007/s12541-024-00962-4
18. A. Jiang, M. Qi, J. Xiao, Preparation, structure, properties, and application of copper nitride (Cu_3N) thin films: a review. J. Mater. Sci. Technol. **34**, 1467–1473 (2018). https://doi.org/10.1016/j.jmst.2018.02.025
19. C. Gallardo-Vega, W. de la Cruz, Study of the structure and electrical properties of the copper nitride thin films deposited by pulsed laser deposition. Appl. Surf. Sci. **252**, 8001–8004 (2006). https://doi.org/10.1016/j.apsusc.2005.10.007
20. K. Matsuzaki, K. Harada, Y. Kumagai, S. Koshiya, K. Kimoto, S. Ueda, M. Sasase, A. Maeda, T. Susaki, M. Kitano, F. Oba, H. Hosono, High-mobility p-type and n-type copper nitride semiconductors by direct nitriding synthesis and in silico doping design. Adv. Mater. (2018). https://doi.org/10.1002/adma.201801968
21. M.I. Rodríguez-Tapiador, J.M. Asensi, M. Roldán, J. Merino, J. Bertomeu, S. Fernández, Copper nitride: a versatile semiconductor with great potential for next-generation photovoltaics. Coatings **13**, 1094 (2023). https://doi.org/10.3390/coatings13061094
22. M.L. Huang, Z. Cai, Y.Z. Wu, S.G. Lu, B.S. Luo, Y.H. Li, Metallic coloration on polyester fabric with sputtered copper and copper oxides films. Vacuum **178**, 109489 (2020). https://doi.org/10.1016/J.VACUUM.2020.109489
23. M.L. Huang, Y.Z. Wu, Z.K. Liu, S.G. Lu, Metallic coloration and multifunctional preparation on fabrics via nitriding reactive sputtering with copper and titanium targets. Vacuum **202**, 111177 (2022). https://doi.org/10.1016/J.VACUUM.2022.111177
24. C.A. Figueira, G. Del Rosario, D. Pugliese, M.I. Rodríguez-Tapiador, S. Fernández, Effect of argon on the properties of copper nitride fabricated by magnetron sputtering for the next generation of solar absorbers. Materials **15**(24), 8973 (2022). https://doi.org/10.3390/ma15248973
25. M.I. Rodríguez-Tapiador, A. Jiménez-Suárez, A. Lama, N. Gordillo, J.M. Asensi, G. del Rosario, J. Merino, J. Bertomeu, A. Agarwal, Effects of deposition temperature and working pressure on the thermal and nanomechanical performances of stoichiometric Cu3N: an adaptable material for photovoltaic applications. Nanomaterials **13**, 2950 (2023)
26. G.H. Yue, P.X. Yan, J.Z. Liu, M.X. Wang, M. Li, X.M. Yuan, Copper nitride thin film prepared by reactive radio-frequency magnetron sputtering. J. Appl. Phys. **98**(10), 103506 (2005). https://doi.org/10.1063/1.2132507
27. J. Xiao, Y. Li, A. Jiang, Structure, optical property and thermal stability of copper nitride films prepared by reactive radio frequency magnetron sputtering. J. Mater. Sci. Technol. **27**(5), 403–407 (2011). https://doi.org/10.1016/S1005-0302(11)60082-0
28. G.K. Williamson, R.E. Smallman, Iii. Dislocation densities in some annealed and cold-worked metals from measurements on the x-ray Debye-Scherrer spectrum. Philos. Mag. **1**(1), 34–46 (1956). https://doi.org/10.1080/14786435608238074
29. M.I. Rodríguez-Tapiador, J.M. Mánuel, E. Blanco, E. Márquez, N. Gordillo, R. Sainz, J. Merino, S. Fernández, Effects of N_2 concentration on structural, morphological, and optoelectronic properties of Cu_3N films fabricated by RF magnetron sputtering for photodetection applications. Mater. Sci. Semicond. Process. **188**, 109176 (2025). https://doi.org/10.1016/j.mssp.2024.109176
30. Y. Du, A.L. Ji, L.B. Ma, Y.Q. Wang, Z.X. Cao, Electrical conductivity and photoreflectance of nanocrystalline copper nitride thin films deposited at low temperature. J. Cryst. Growth **280**, 490–494 (2005). https://doi.org/10.1016/j.jcrysgro.2005.03.077
31. D. Miao, H. Hu, A. Li, S. Jiang, S. Shang, Fabrication of porous and amorphous TiO2 thin films on flexible textile substrates. Ceram. Int. **41**(7), 9177–9182 (2015). https://doi.org/10.1016/j.ceramint.2015.03.080
32. Y. Ju, L. Ai, X. Qi, J. Li, W. Song, Review on hydrophobic thin films prepared using magnetron sputtering deposition. Materials **16**(10), 3764 (2023). https://doi.org/10.3390/ma16103764
33. K.V. Rani, B. Sarma, A. Sarma, Plasma sputtering process of copper on polyester/silk blended fabrics for preparation of multifunctional properties. Vacuum **146**, 206–215 (2017). https://doi.org/10.1016/j.vacuum.2017.09.036